NATIONAL ADVISORY COMMITTEE FOR AERONAUTICS

WARTIME REPORT

ORIGINALLY ISSUED
June 1942 as
Memorandum Report

TESTS OF FOUR MODELS REPRESENTING INTERMEDIATE SECTIONS OF THE XB-33 AIRPLANE INCLUDING SECTIONS WITH SLOTTED FLAP AND AILERONS

By Ira H. Abbott

Langley Memorial Aeronautical Laboratory
Langley Field, Va.

NACA

WASHINGTON

NATIONAL ADVISORY COMMITTEE FOR AERONAUTICS

MEMORANDUM REPORT

for

Army Air Forces, Materiel Command

TESTS OF FOUR MODELS REPRESENTING INTERMEDIATE SECTIONS OF THE XB-33 AIRPLANE INCLUDING SECTIONS WITH SLOTTED FLAP AND AILERONS

By Ira H. Abbott

INTRODUCTION

At the request of the Materiel Command, Army Air Forces, tests were made in the Langley two-dimensional tunnel of four models submitted by the Glenn L. Martin Company as intermediate sections of the wing of the XB-33 airplane. The models were of 24-inch chord and were constructed of wood with pressure-distribution orifices. The models were identified by station numbers of 85, 250, 430, and 620, respectively, of the wing of the XB-33 airplane. This wing is formed by fairing between an NACA 65,2-222 $a = 1$ root section and an NACA 65,2-415 $a = 0.5$ tip section.

Sections number 85 and 430 were represented by simple airfoil models without flaps.

Section number 250 was represented by a model complete with slotted flap. Tests on this section included lift, drag, and pressure-distribution measurements with various flap deflections. Several alterations of the flap and several alternate flap positions were tested to obtain improved flap characteristics.

Section number 620 was represented by a model with alternate ailerons of the Frise and internal-balance types. Tests of this section included lift, drag, hinge-moment and pressure-distribution measurements with various deflections of each aileron. The aileron hinge moments were obtained by integration of pressure distributions over the ailerons.

Most of the data were obtained at a Reynolds number of approximately 6 million although some data were obtained at approximately 3 and 10 million. The large number of pressure-distribution diagrams obtained are not presented in this report.

METHODS[1]

Lift and drag measurements were made by the methods described in reference 1. The moment coefficients presented were obtained by integration of the diagrams obtained by plotting the pressures against the projection of the orifice locations on the chord line. These moment coefficients accordingly do not contain the component of moment associated with the chord force.

Aileron hinge-moment coefficients were obtained from pressure-distribution measurements. In this case two diagrams were integrated to obtain each moment coefficient, the pressures being plotted, respectively, against the orifice projections on the reference line and on a line perpendicular to the reference line. In some cases, especially for negative deflections of the Frise aileron, the orifices were not located sufficiently close together to define adequately the pressure distribution thus introducing a possible error in the hinge-moment coefficients.

---

[1] At the time this report was originally published, some of the corrections required for reducing the test data to free-air conditions had not been determined. The values of section lift coefficient c_l (figs. 1 to 4) for the models corresponding to stations 85 and 430 should be corrected by the equation

$$c_{l_{(\text{corrected})}} = 0.965\, c_l + 0.007$$

The section lift coefficients of the model corresponding to station 250 (figs. 6 to 3 and figs. 15 to 18) should be corrected by the equation

$$c_{l_{(\text{corrected})}} = 0.965\, c_l + K$$

where the values of K are 0.005, 0.02, 0.03, and 0.04 for flap deflections of 0°, 20°, 30°, and 40°, respectively.

The section lift coefficients of the model corresponding to station 620 (figs. 20 to 22 and figs. 24 to 26) should be corrected by the equation

$$c_{l_{(\text{corrected})}} = 0.965\, c_l + 0.030\, c_{l_{\alpha=1^\circ}}$$

where $c_{l_{\alpha=1^\circ}}$ is the section lift coefficient at an angle of attack of 1°.

RESULTS AND DISCUSSION

Stations 85 and 430.- Lift and drag data obtained for the models representing wing sections at stations 85 and 430 are presented in figures 1 to 4. The lift characteristics of the two sections are similar except that the thinner outboard section shows an appreciably higher maximum lift coefficient than the inboard section at the highest Reynolds number (figs. 1 and 3). Also presented in figures 1 and 3 are the moment coefficients associated with the normal-force coefficients as obtained from pressure distributions. The minimum drag coefficients of the two sections (figs. 2 and 4) are nearly the same. Outside the low-drag range the drag coefficients increase rapidly with lift coefficient. Recent work (reference 2) indicates that sections as thick as that at station 85 are critical to separation when accidentally roughened and that such sections may have drag coefficients so high (fig. 3 of reference 2) when rough as to seriously effect flight at cruising lift coefficients. These data indicate the desirability of reducing the thickness ratio of the root section.

Station 250.- The model which represented the wing section at station 250 was equipped with a slotted flap as shown in figure 5. The flap arrangement was such as to leave a gap in the lower surface when retracted. Lift and drag characteristics for the model are presented in figures 6 and 7 for flap deflections of 0°, 20°, 30°, and 40°. For the flap-retracted condition, tests were made with the slot sealed to prevent flow through it without change in external contour.

The maximum lift coefficients for flap deflections of 30° and 40° were nearly the same, about 2.7 (fig. 6). The drag with the gap open, flap retracted, was high (fig. 7) and the data showed considerable scatter which is thought to be associated with spanwise flow of low-energy air in the gap into or away from the survey plane, even though dams were placed in the gap to prevent such flow from extending very far along the span. This condition resulted in variation of the measured drag coefficients along the span. The drag curve in figure 7 is dotted to indicate the estimated drag coefficients.

Several alternate flap positions were tested with the flap deflected 30° to study the effect of flap position on maximum lift. The results are presented in figure 8. The flap was moved parallel and perpendicular to the airfoil chord line from the original position by amounts shown in figure 8 in fractions of the airfoil chord. The best position was found to be 0.01c higher than and 0.005c aft of the original position. The maximum lift coefficient in this position was 2.8.

Several modifications of the flap as shown in figures 9 to 13 were tested to determine their effect.

Condition A (fig. 9) represented a buffer of rubber or other material inserted in the slot in such a manner as to seal it with the flap retracted. This modification caused little change in lift characteristics (fig. 14) and small changes in drag (fig. 7) with the flap deflected 30°.

Condition B (fig. 10) represented a condition with a filler block to fair out the gap in the lower surface with flap retracted. This condition was represented by filling the gap with modeling clay with flap retracted and by a properly shaped piece of wood with flap deflected. This condition did not change the lift characteristics with flap retracted (fig. 6) and reduced the drag coefficient, flap retracted, by about 0.001 in the low-drag range as compared with the original condition, gap open and slot sealed (fig. 7). The drag in this condition was practically that to be expected for the plain airfoil. The maximum lift, however, was very low with flap deflected in this condition (fig. 14), indicating the need of a door to close the gap with this type of flap.

Conditions C and D (figs. 11 and 12) represent attempts to reduce the drag with flap neutral without the use of a door by reducing the size of the gap. The results showed that the filler blocks did not reduce the drag, flap retracted (fig. 15), and caused losses in maximum lift coefficient (fig. 14).

Condition E (fig. 13) was a modification of the slot entry by cutting it back to an angle of 53° from the chord line with no radius at the intersection with the lower surface. Condition F was the same as Condition E with the addition of a shutter such as might be used to revolve and close the gap with the flap retracted. These modifications were tested with the flap deflected 30° in the position previously found to be best (fig. 8). The lift characteristics obtained are shown in figure 16. The maximum lift obtained with either modification was about the same as for the original condition with the flap in the best position (fig. 8). The drag characteristics of Condition E, with flap deflected 30°, are similar to those for the original condition (figs. 7 and 17), but the addition of the shutter (Condition F) caused an appreciable increase in drag at lift coefficients below about 1.7 (fig. 17). The scale effects on the lift characteristics with flap retracted and deflected 30° in the original condition, but in the best position found, are shown by the lift curves of figure 18. The maximum lift coefficient, flap deflected, increased from about 2.8 to 2.9 with an increase in Reynolds number from about 6 to 10 million.

Station 620.- The model representing station 620 was fitted with two ailerons, one of which was of the Frise type (fig. 19). Lift and drag characteristics of this model with various deflections of the Frise aileron are presented in figures 20 and 21. Hinge moments obtained from pressure-distribution measurements and cross plots of lift coefficients against aileron deflection at various angles of attack are shown in figure 22. Complete hinge-moment coefficient curves were obtained only at angles of attack of 2.2° and 14.5°. The accuracy of the hinge-moment coefficients is somewhat doubtful, especially for negative aileron deflections, because the aileron contained too few pressure orifices to adequately describe the pressure distributions.

The other aileron was of the internal-balance type (fig. 23), and data similar to that obtained for the Frise aileron were originally obtained before test of the Frise aileron. The model was later reassembled with the internal-balance aileron and retested to obtain the more nearly complete data presented in figures 24 to 26. The accuracy of the hinge-moment data for this aileron is believed to be better than for the Frise aileron because the pressure distributions were better described by the pressure orifices.

The hinge-moment coefficients presented for the internal-balance aileron contain an estimate of the balancing moment resulting from the seal or curtain. This moment was assumed to be equal to that resulting from the applications of a force at the point of attachment of the curtain to the aileron. This force was assumed to act at an arm of $0.504c_A$ (fig. 23) and to be equal to

$$\frac{.18c_A}{2}\Delta p$$

where Δp was the pressure difference across the seal (fig. 23).

The two ailerons are of about equal effectiveness (figs. 20, 22, 24, and 26). The shift of the lift curve for the internal-balance aileron as compared with the Frise aileron (figs. 20 and 24) is ascribed to warpage of the model before the retest of the internal-balance aileron. The first tests with this aileron did not show such a shift. It is thought that general conclusions, with respect to hinge moments and effectiveness, are not seriously affected by this change in the model.

The drag coefficients for the Frise aileron are about 10-percent higher than for the internal-balance aileron in the low-drag range, aileron neutral (figs. 21 and 25).

The hinge-moment coefficients for the Frise aileron (fig. 22) show the typical tendency to overbalance for negative deflections and rather large unbalancing moments for positive deflections. The hinge-moment coefficients for the internal-balance aileron (fig. 26) are generally smaller than for the Frise aileron and show a slight tendency to overbalance for certain combinations of aileron deflection and angle of attack. The rate of change of hinge-moment coefficients with angle of attack is smaller for the internal-balance aileron than for the Frise aileron.

Langley Memorial Aeronautical Laboratory,
National Advisory Committee for Aeronautics,
Langley Field, Va., June 4, 1942.

REFERENCES

1. Abbott, Ira H., von Doenhoff, Albert E., and Stivers, Louis S.: Summary of Airfoil Data. NACA ACR No. L5C05, 1945.

2. Jacobs, Eastman N., Abbott, Ira H., and Davidson, Milton: Investigation of Extreme Leading-Edge Roughness on Thick Low-Drag Airfoils to Indicate Those Critical to Separation. NACA CB, June 1942.

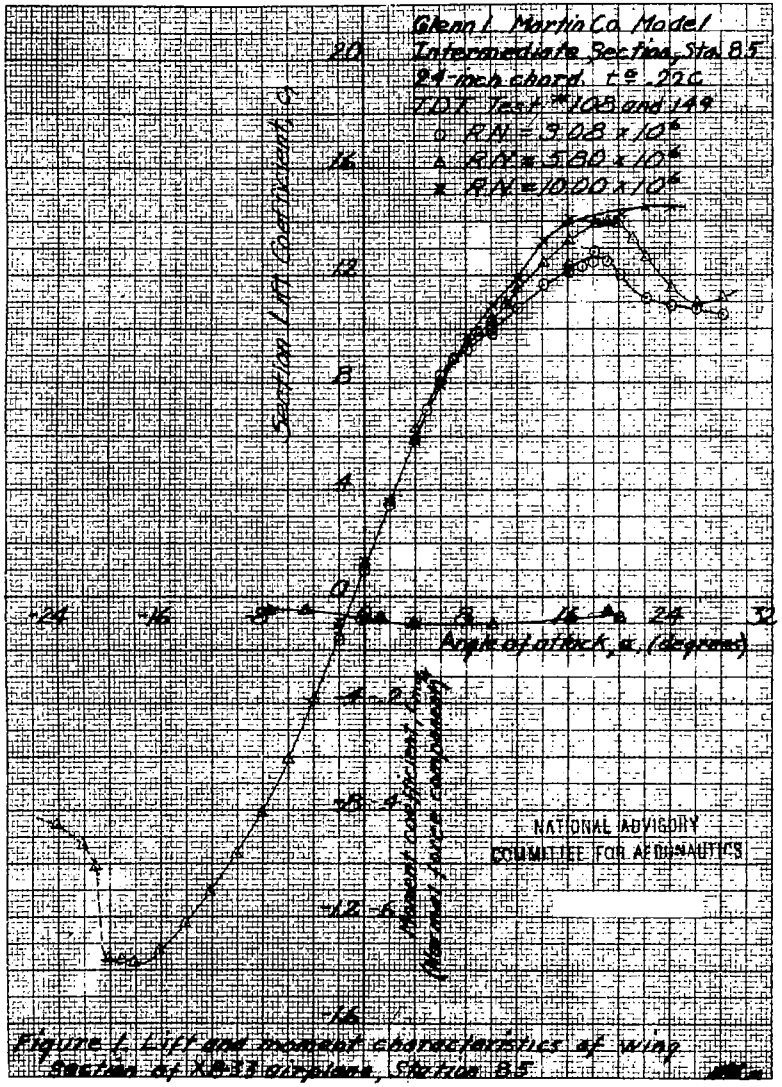

Figure 1. Lift and moment characteristics of wing section of XB-33 airplane, Section 85

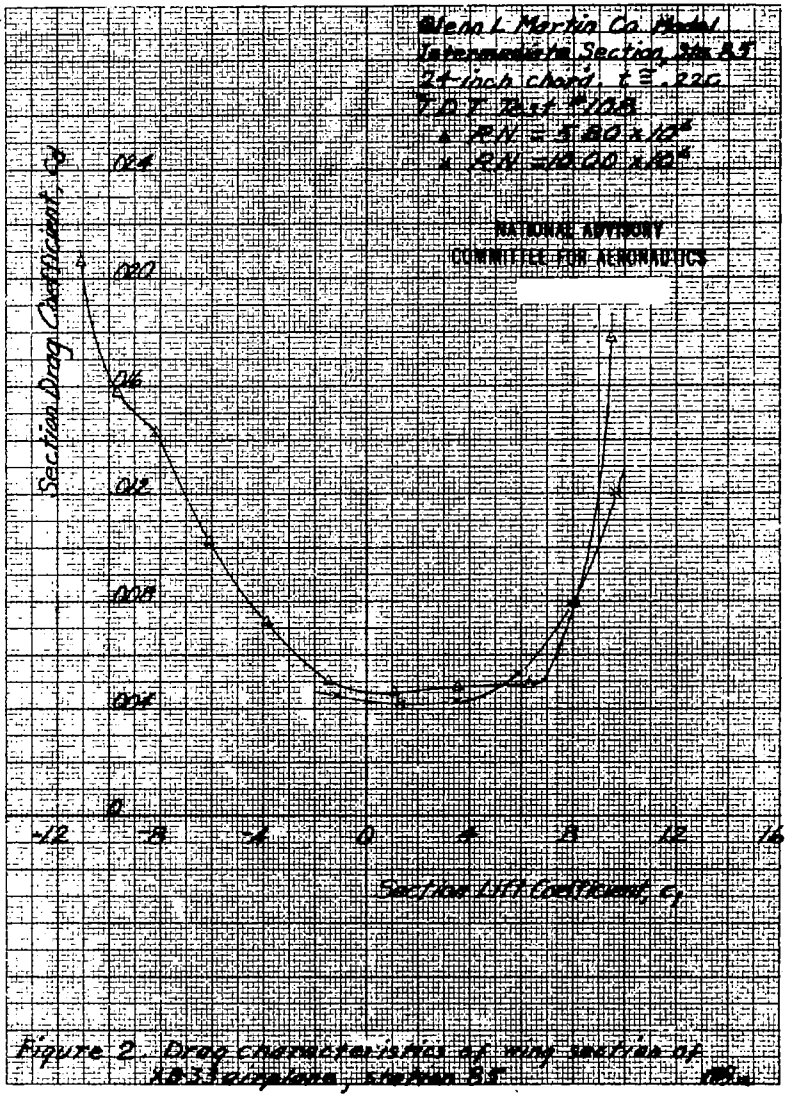

Figure 2. Drag characteristics of wing section of XB-33 airplane, Section 85

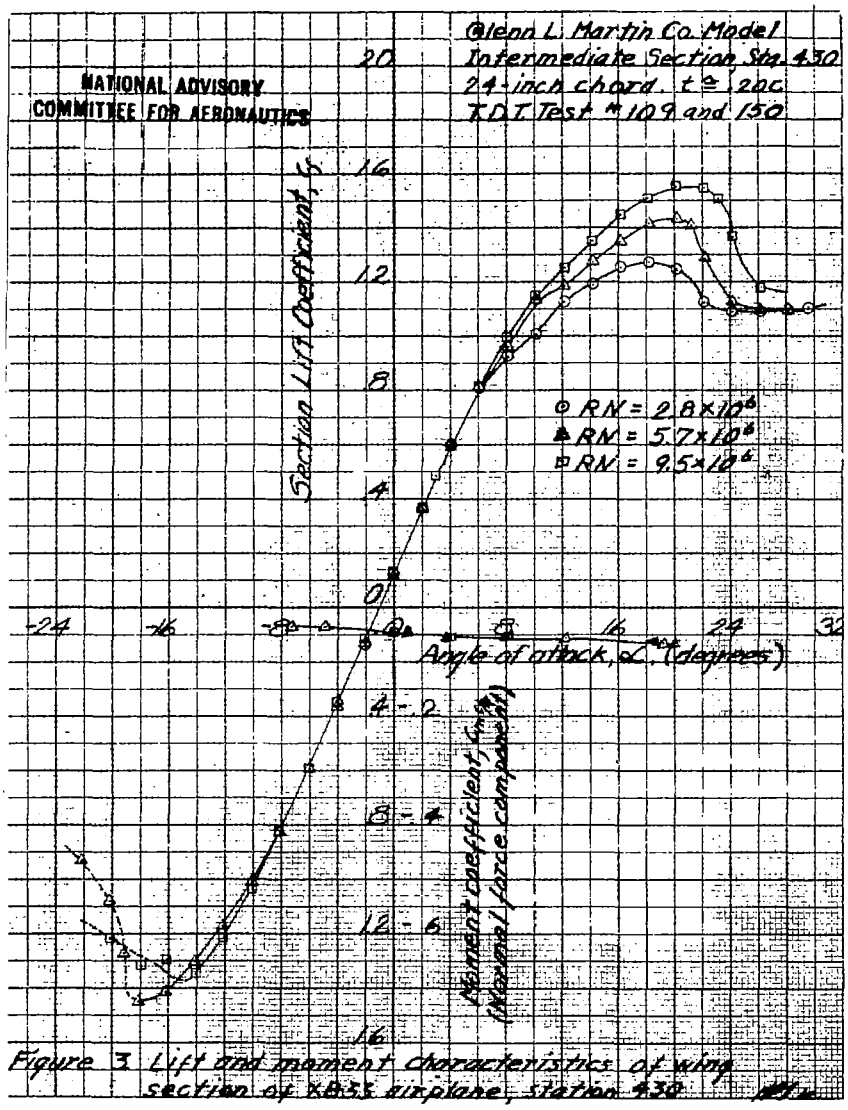

Figure 3 Lift and moment characteristics of wing section of XB-35 airplane, station 430

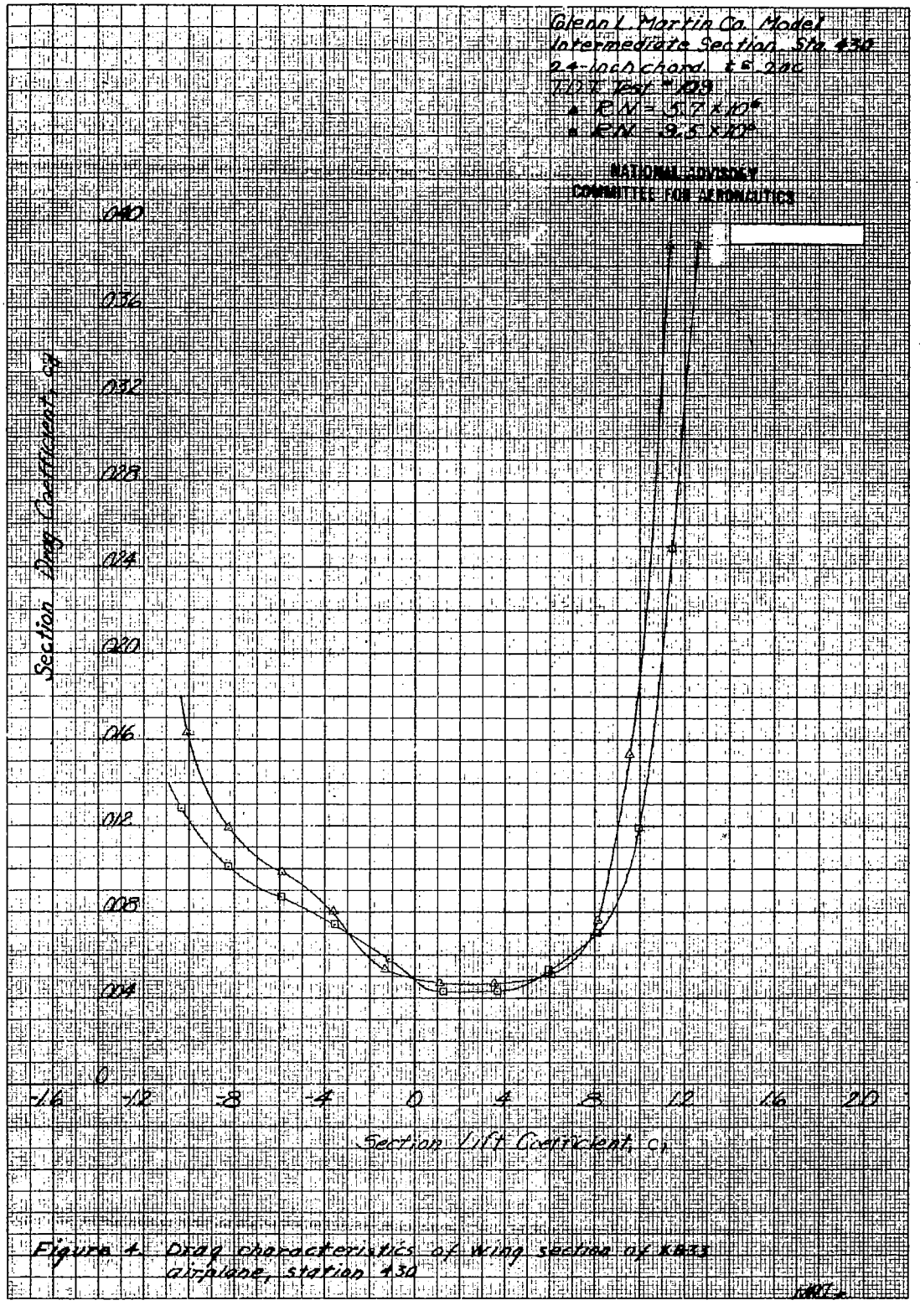

Figure 4. Drag characteristics of wing section of XB-43 airplane, station 130.

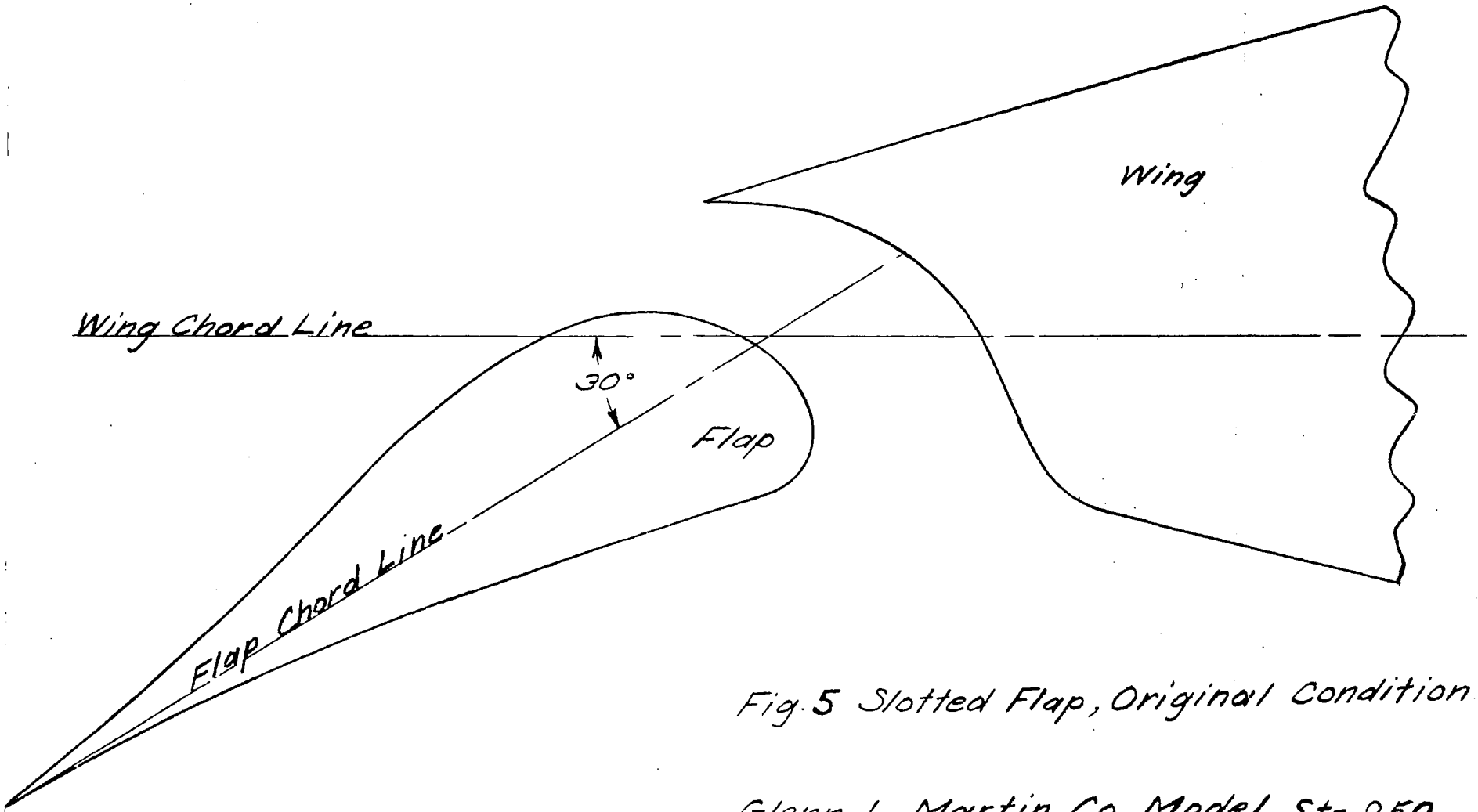

Fig. 5 Slotted Flap, Original Condition

Glenn L. Martin Co. Model, Sta. 250
Intermediate Section XB-33 Wing
Slotted Flap Deflected 30°
Original Condition
Full Model Scale

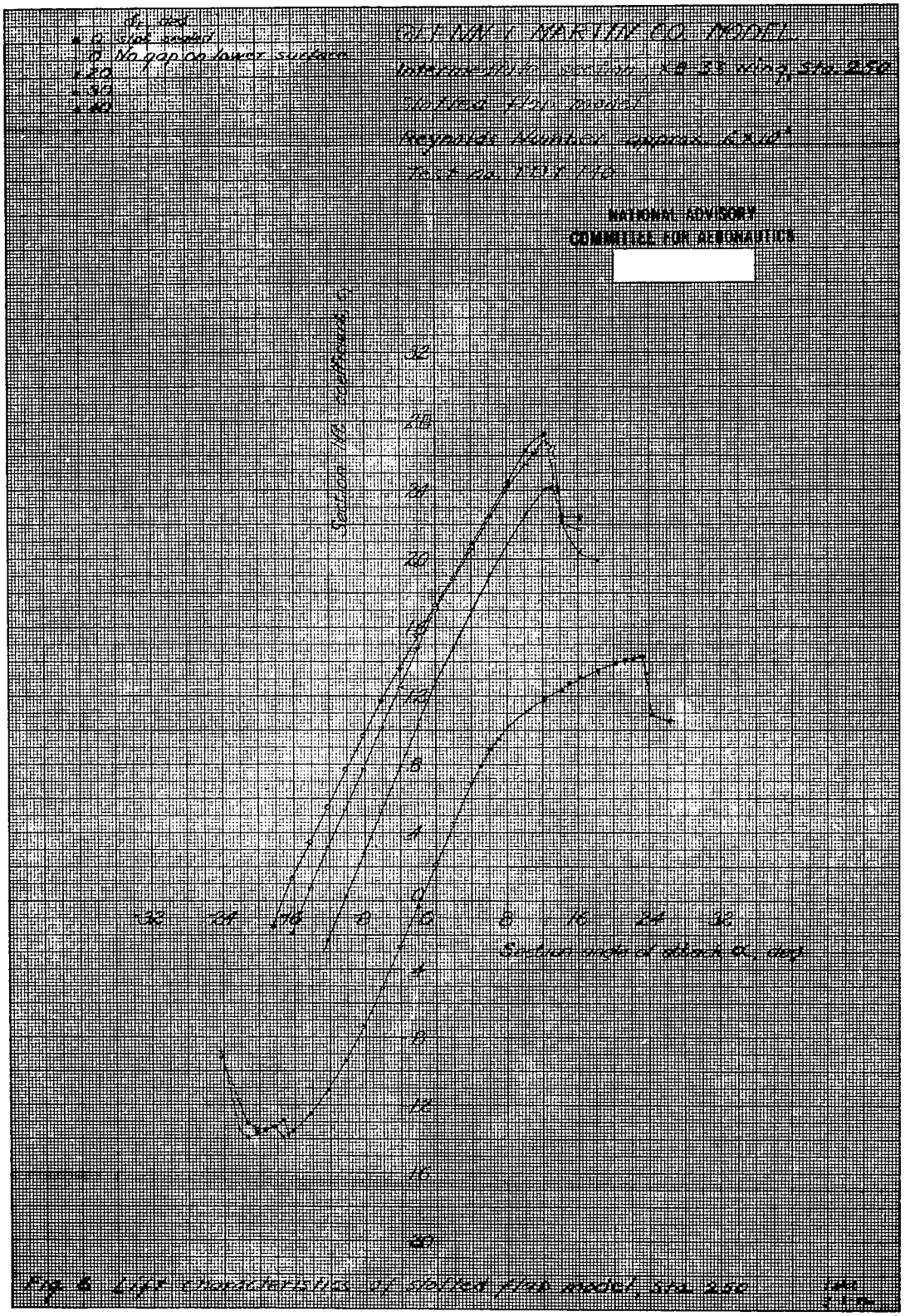

Fig. 6 Lift characteristics of control type model, Sta. 250

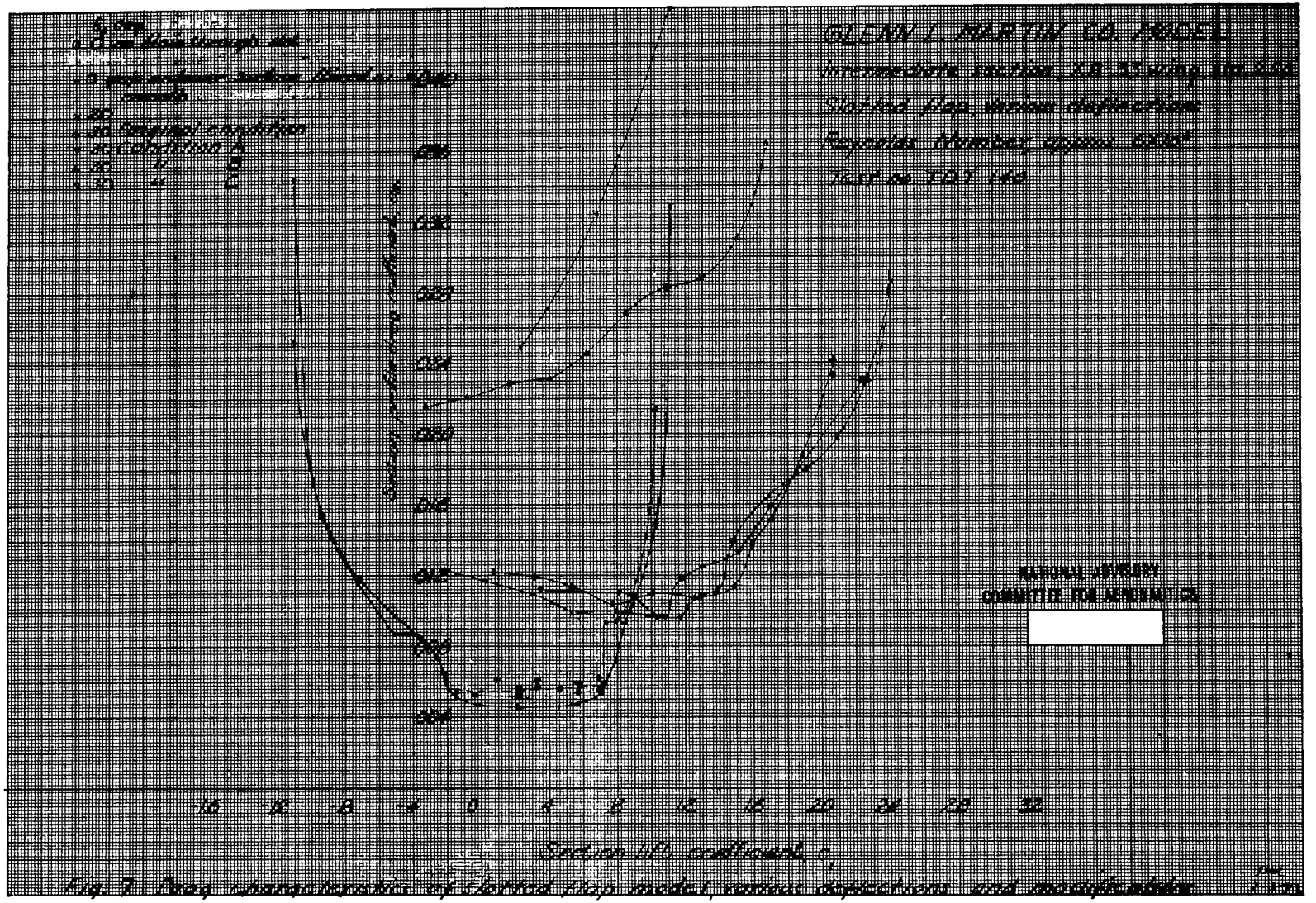

Fig. 7 Drag characteristics of slotted flap model, various deflections and configurations

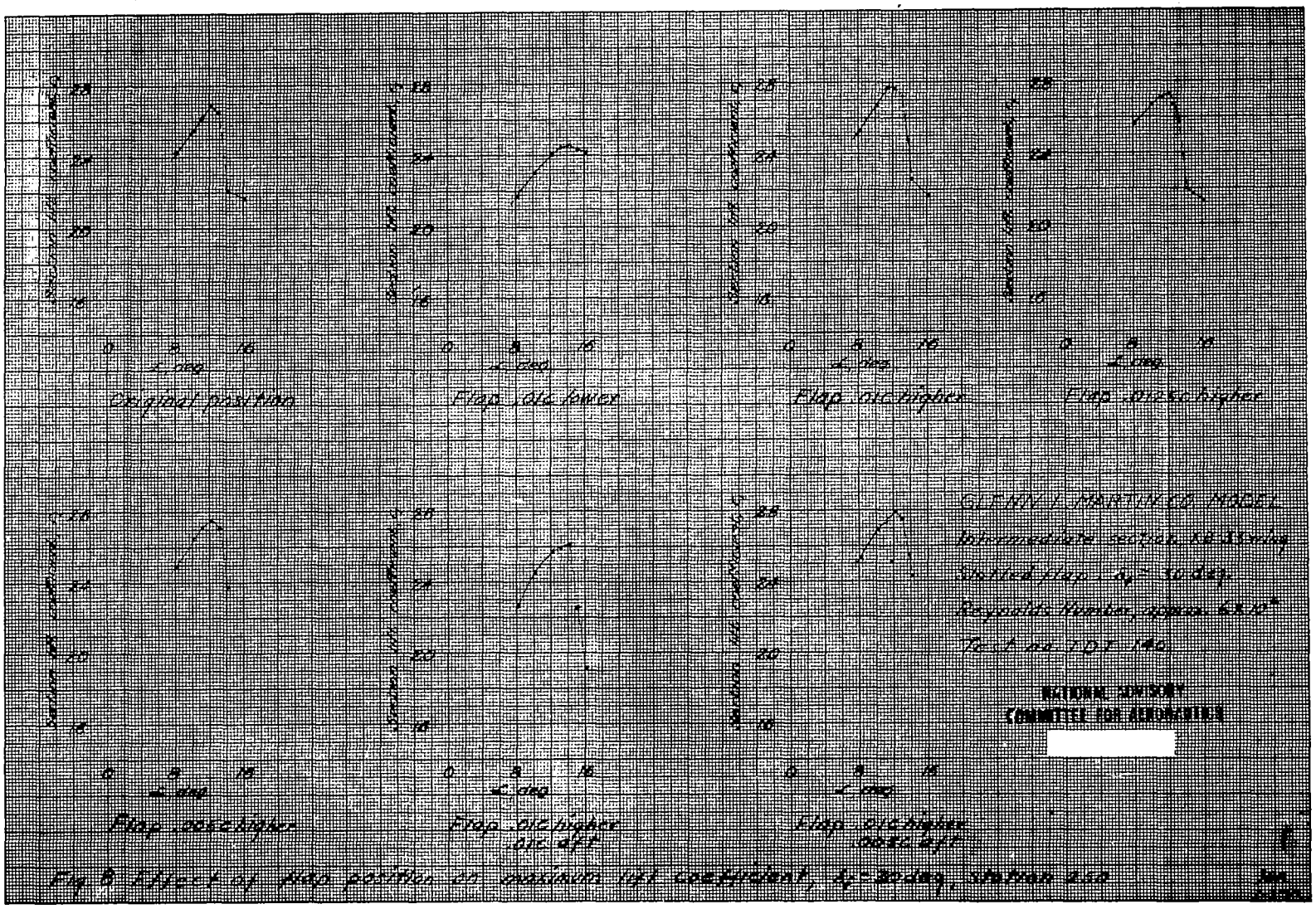

Fig. 8 Effect of flap position on maximum lift coefficient, δ_f = 30 deg., sharp L.E.

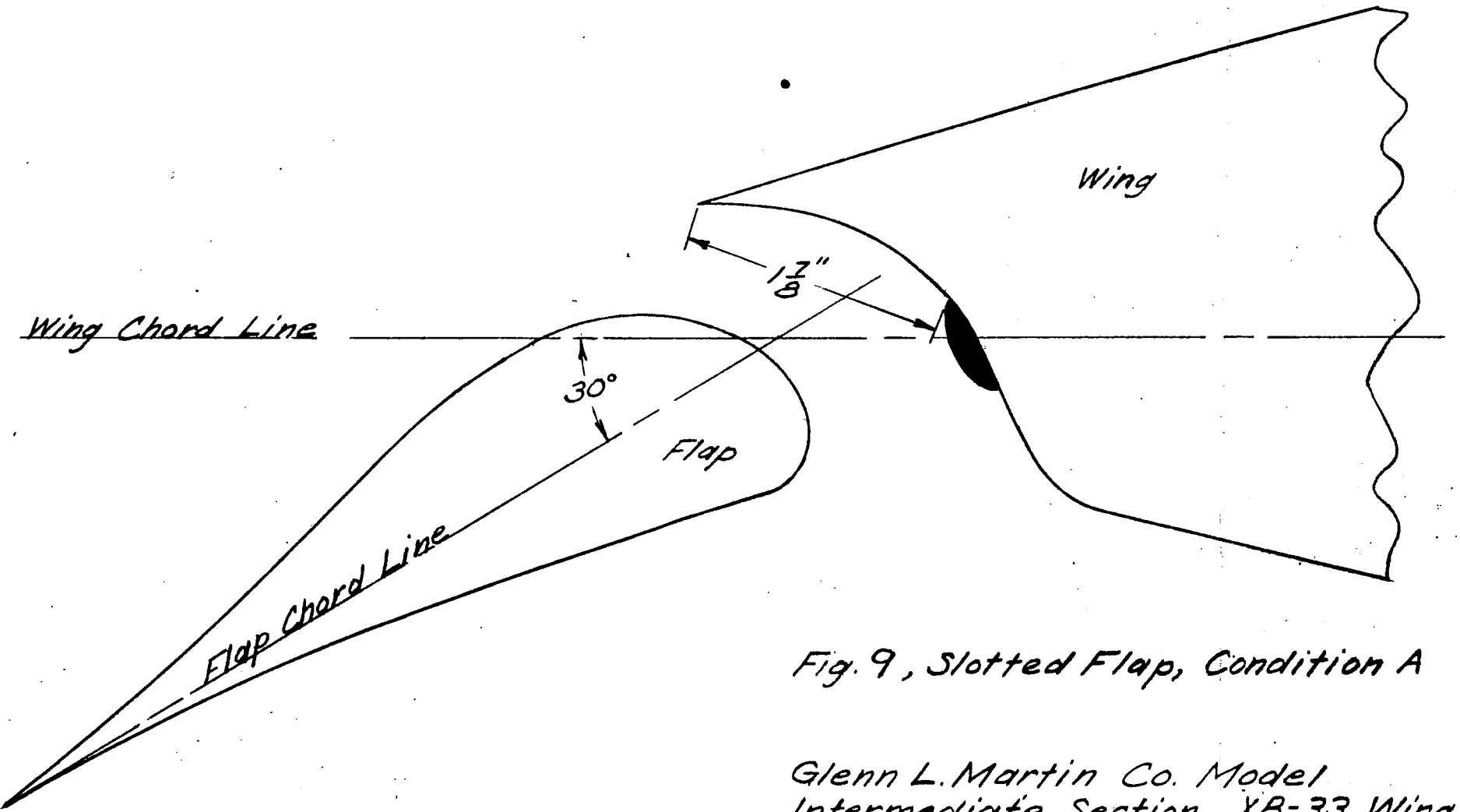

Fig. 9, Slotted Flap, Condition A

Glenn L. Martin Co. Model
Intermediate Section, XB-33 Wing
Slotted Flap Deflected 30°
Modified, Condition A
Full Model Scale

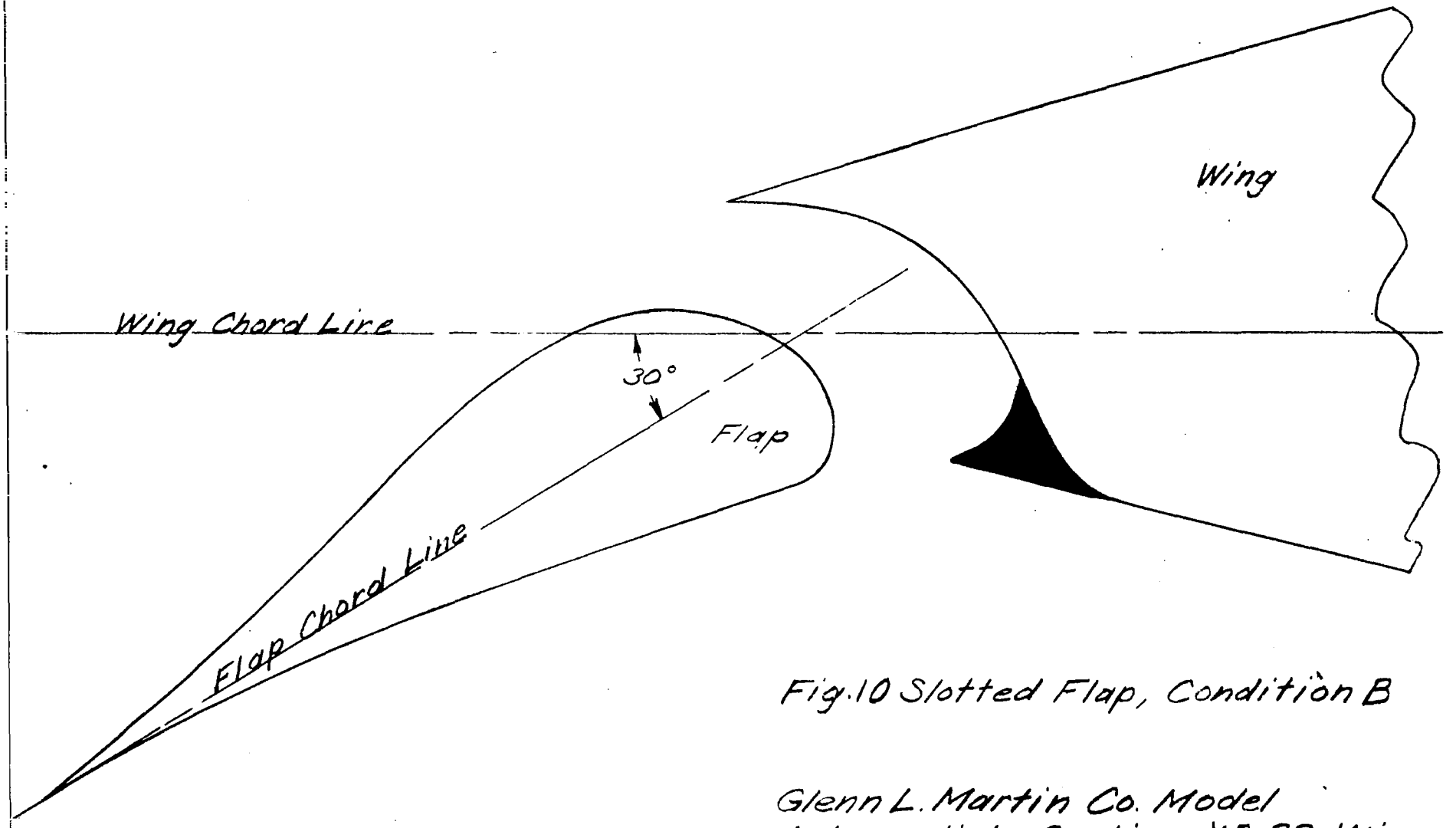

Fig. 10 Slotted Flap, Condition B

Glenn L. Martin Co. Model
Intermediate Section, XB-33 Wing
Slotted Flap Deflected 30°
Modified, Condition B
Full Model Scale

NATIONAL ADVISORY
COMMITTEE FOR AERONAUTICS

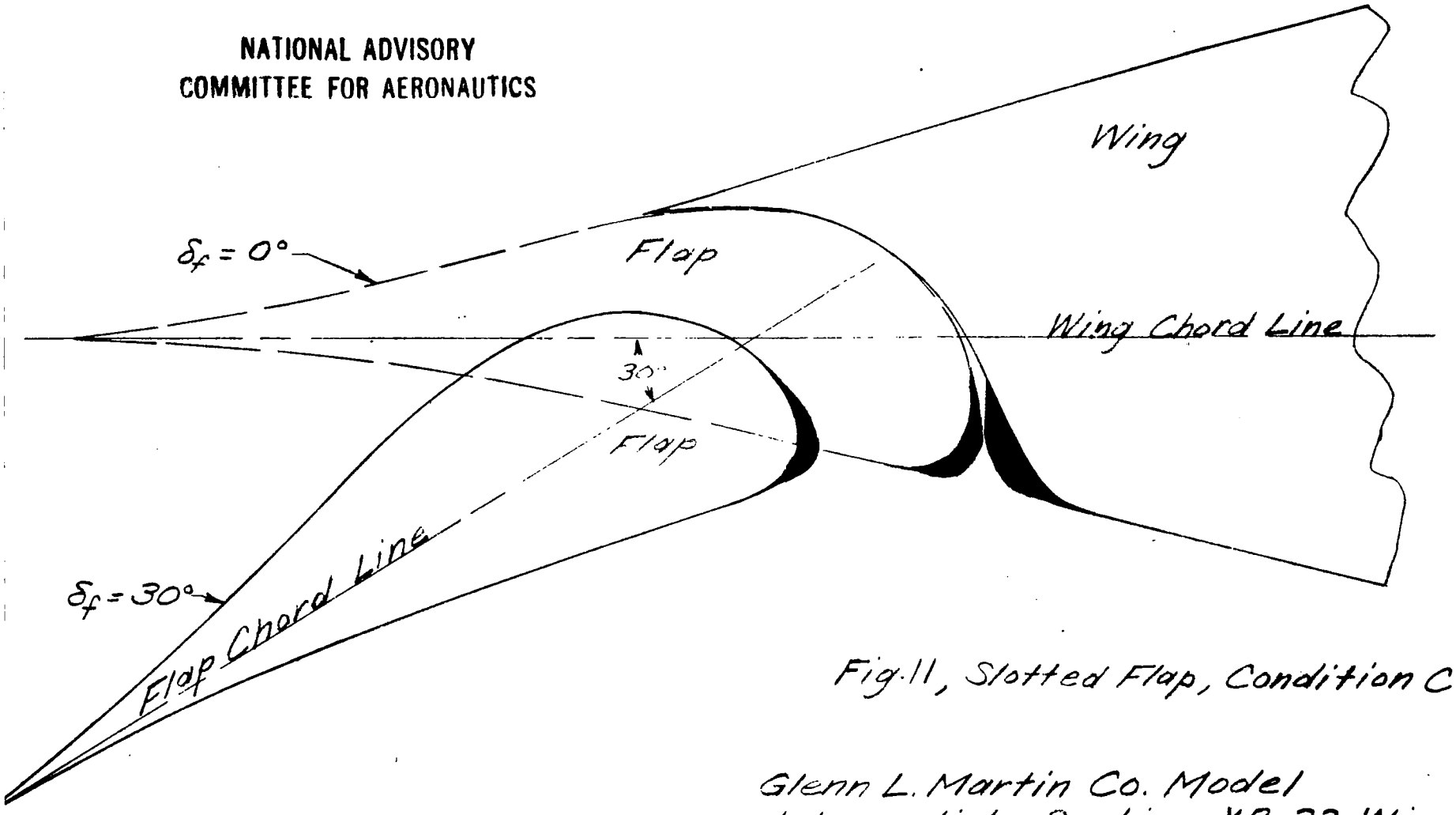

Fig. 11, Slotted Flap, Condition C

Station 250

Glenn L. Martin Co. Model
Intermediate Section, XB-33 Wing
Slotted Flap Deflected 30°
Modified, Condition C
Full Model Scale

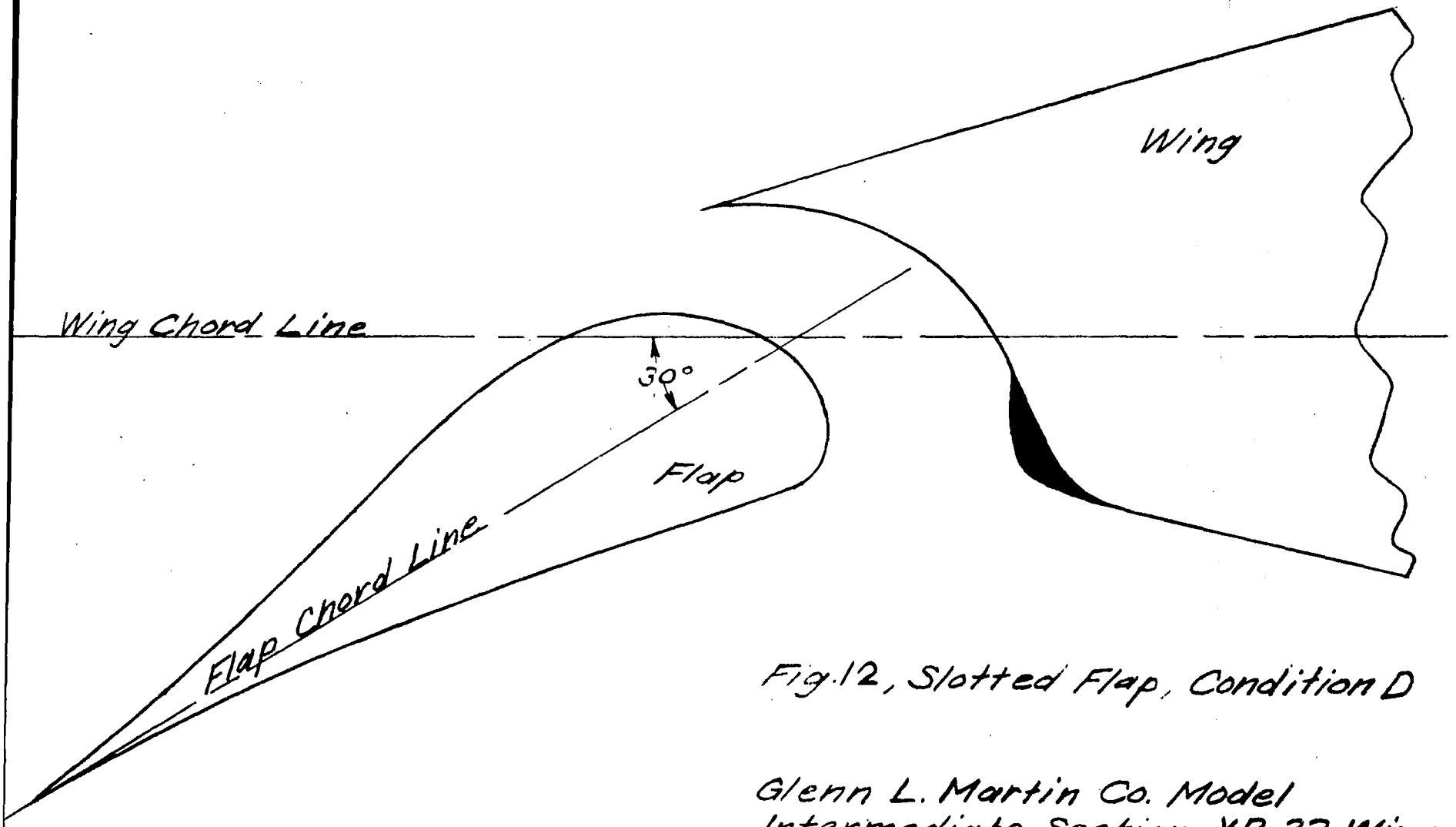

Fig. 12, Slotted Flap, Condition D

Glenn L. Martin Co. Model
Intermediate Section, XB-33 Wing
Slotted Flap Deflected 30°
Modified, Condition D
Full Model Scale

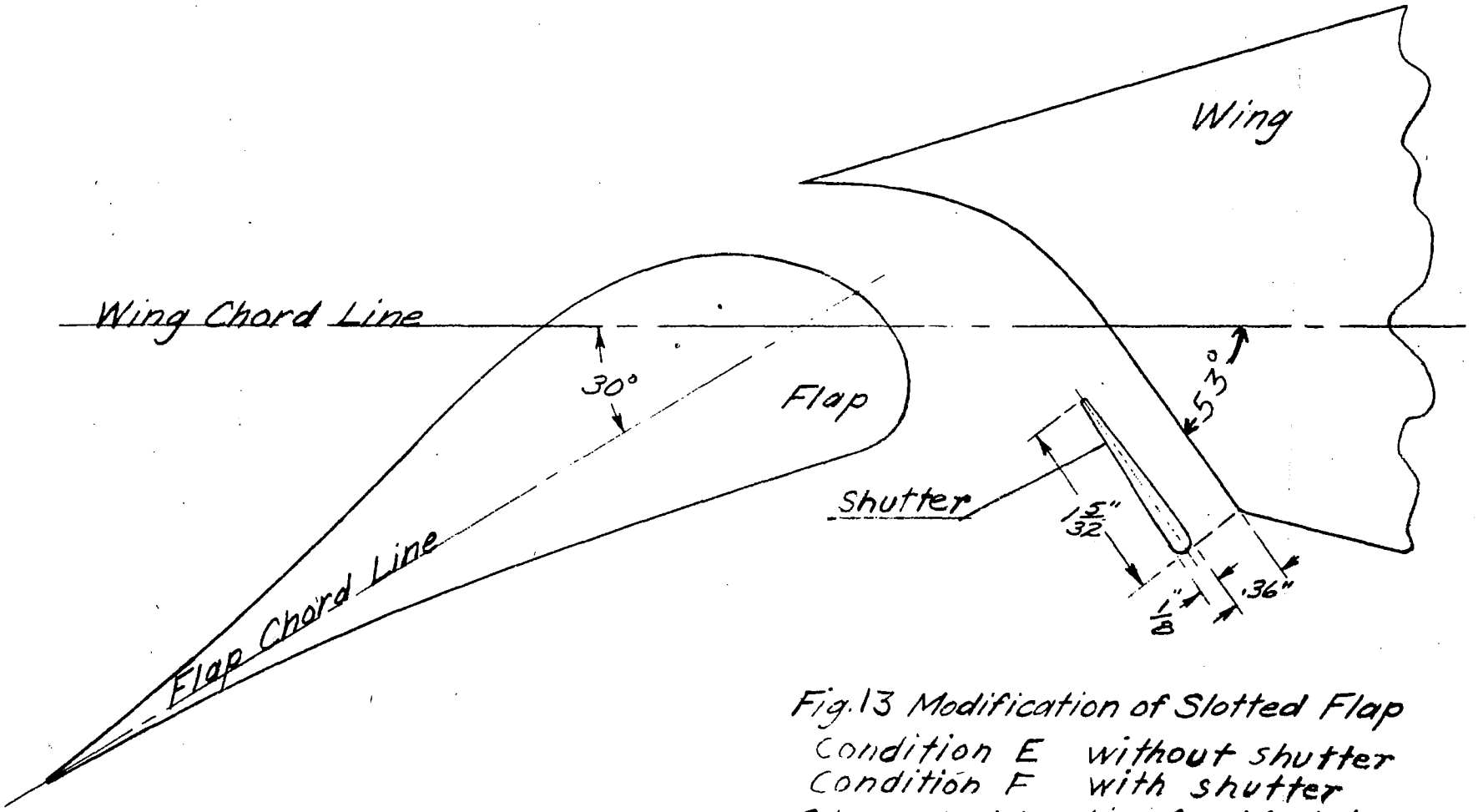

Fig. 13 Modification of Slotted Flap
Condition E without shutter
Condition F with shutter
Glenn L. Martin Co. Model
Intermediate Section, XB-33 Wing
Modification of Slotted Flap
Full Model Scale

Station 250

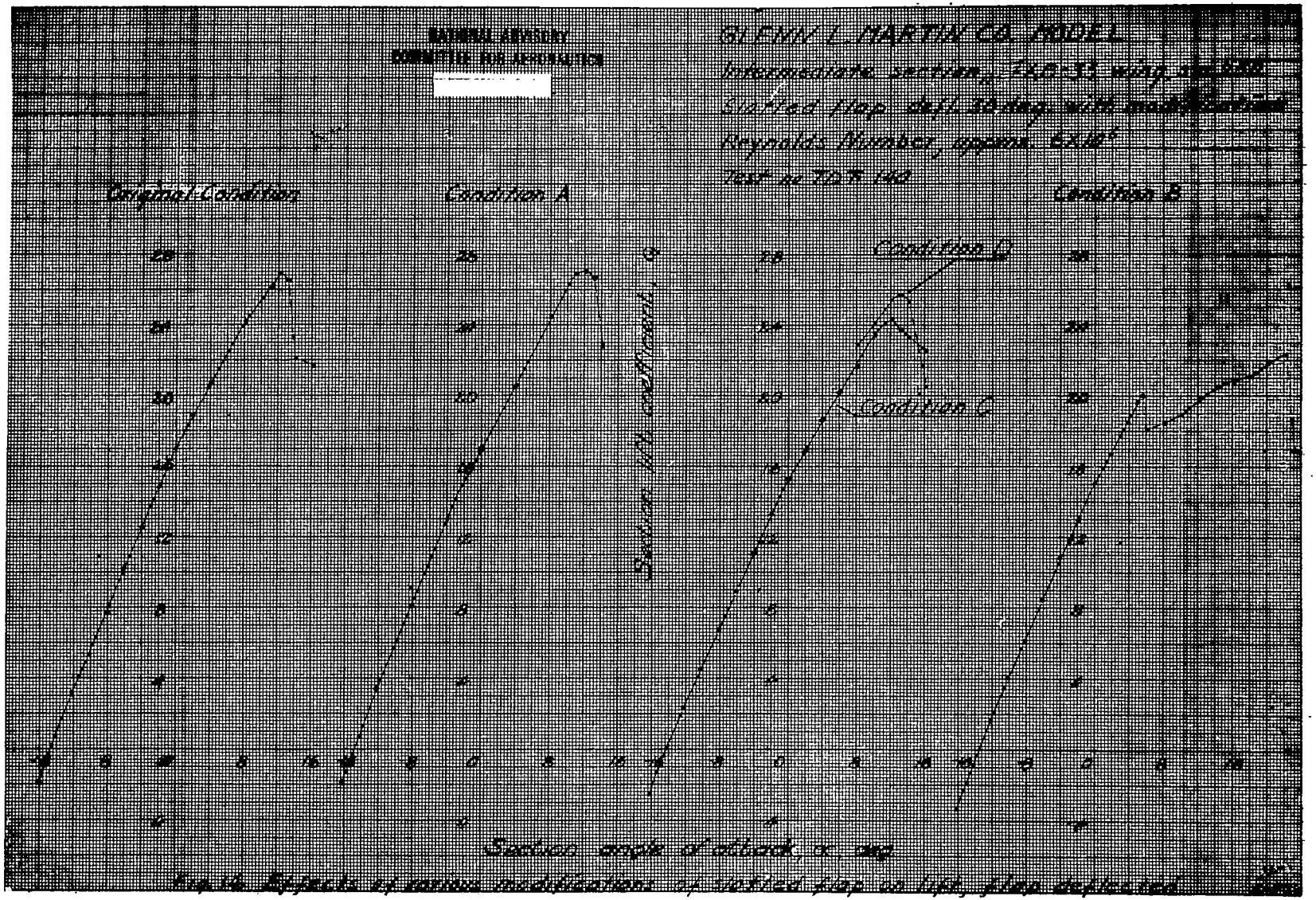

Fig. 16 Effects of various modifications of slotted flap on lift, flap deflected

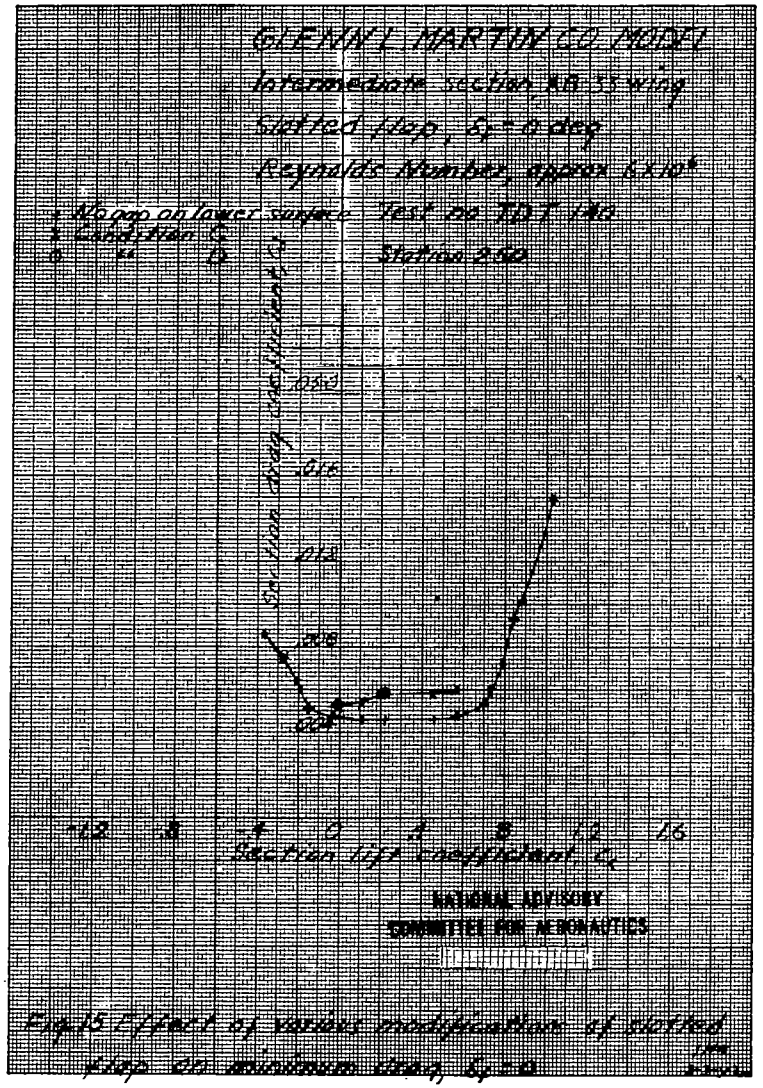

Fig. 15 Effect of various modifications of slotted flap on airfoil section characteristics. δ_f = 0

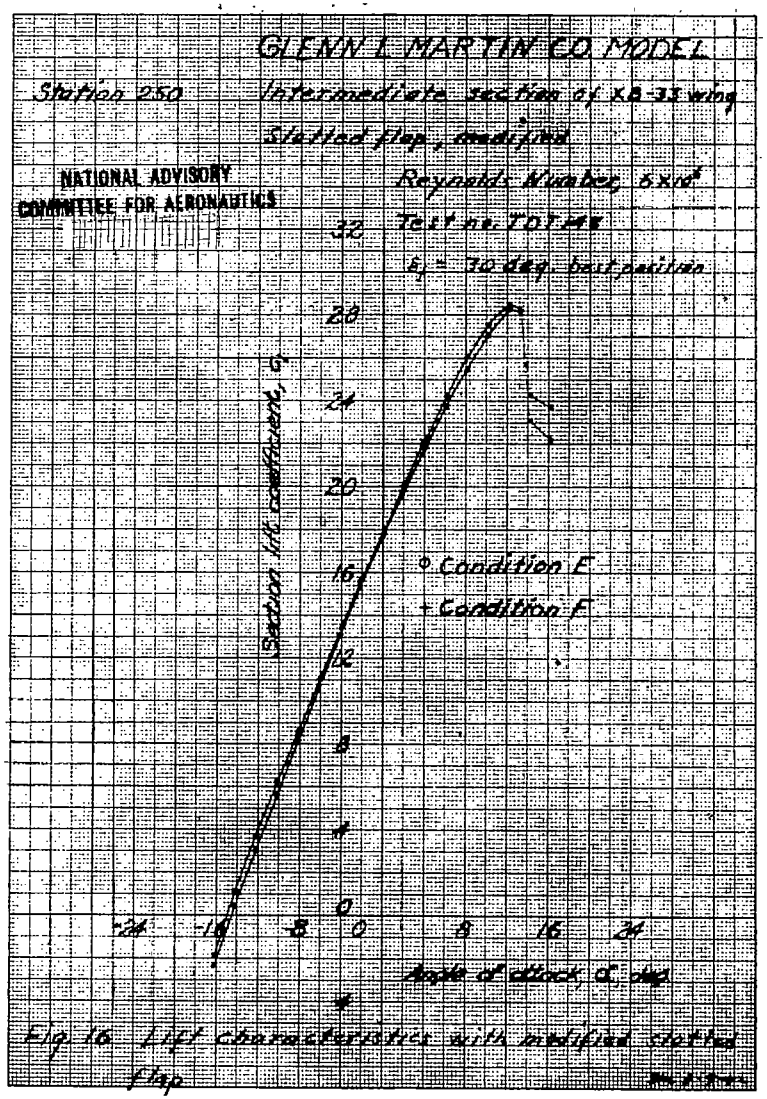

Fig. 16 Lift characteristics with modified slotted flap

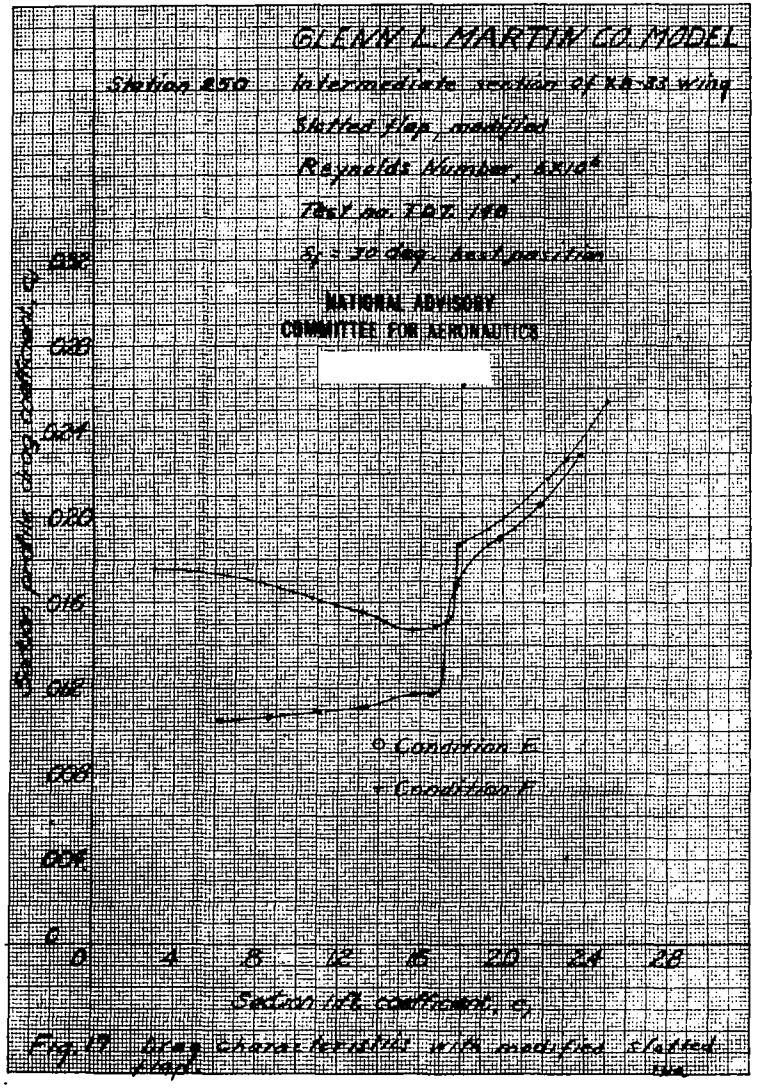

Fig. 17 Drag characteristics with modified slotted flap.

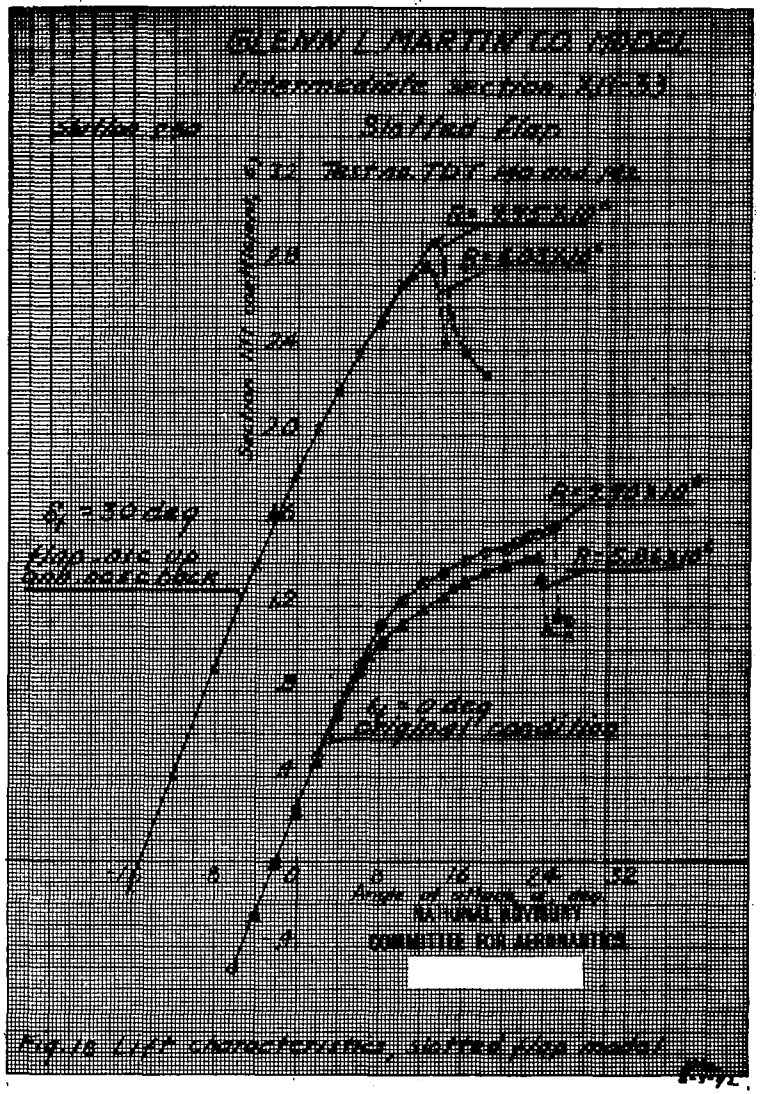

Fig. 18 Lift characteristics, slotted flap model.

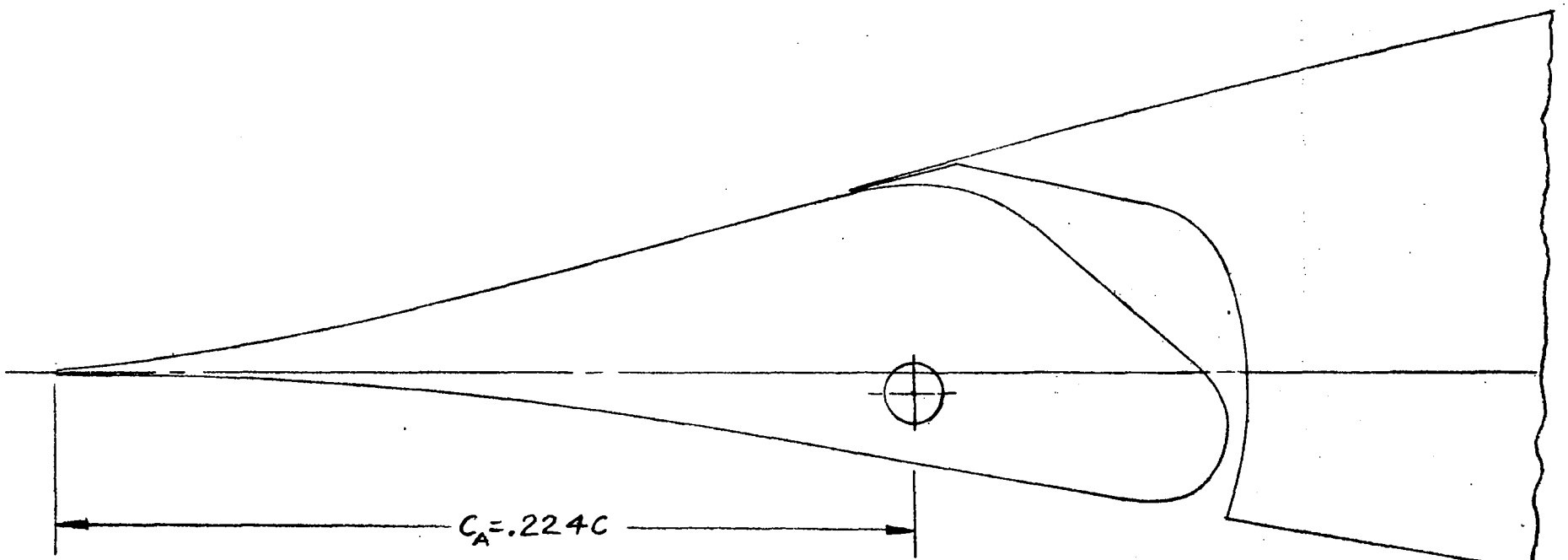

Fig. 19 Frise aileron
Glenn L. Martin Co. Model
Intermediate section, XB-33 wing
Station 620
Full model scale

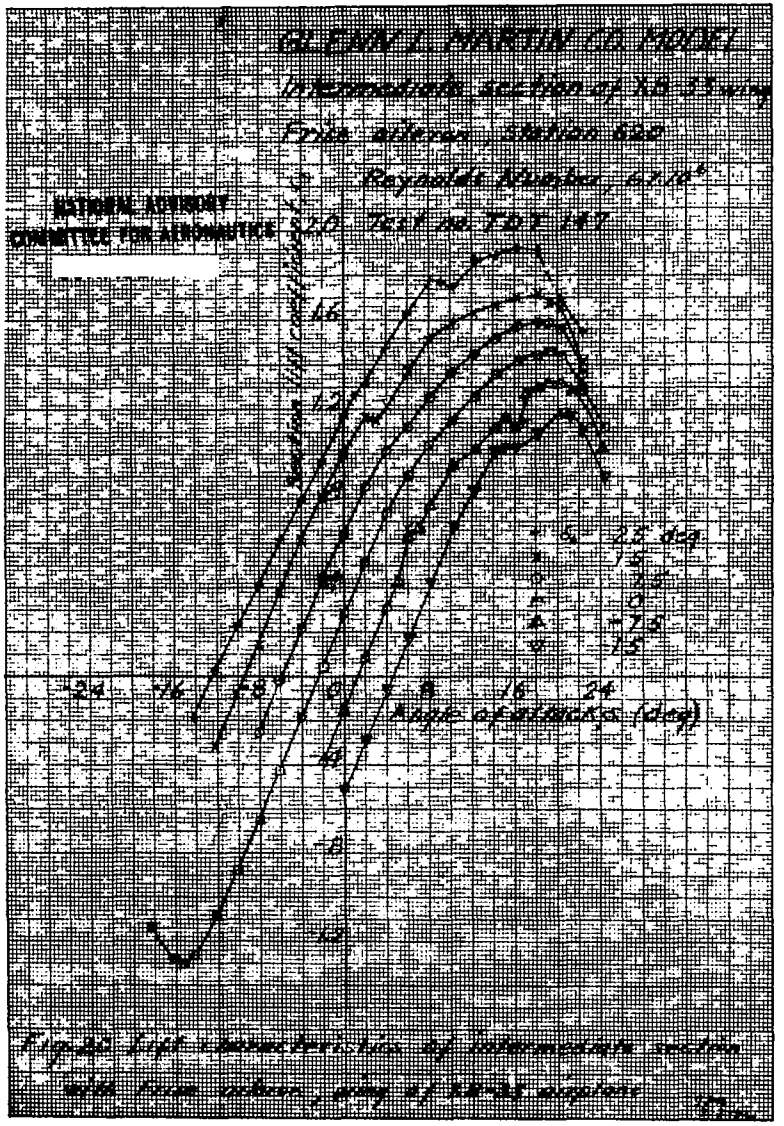

Fig. 20 Lift characteristics of intermediate section with frise aileron, wing of XB-33 airplane.

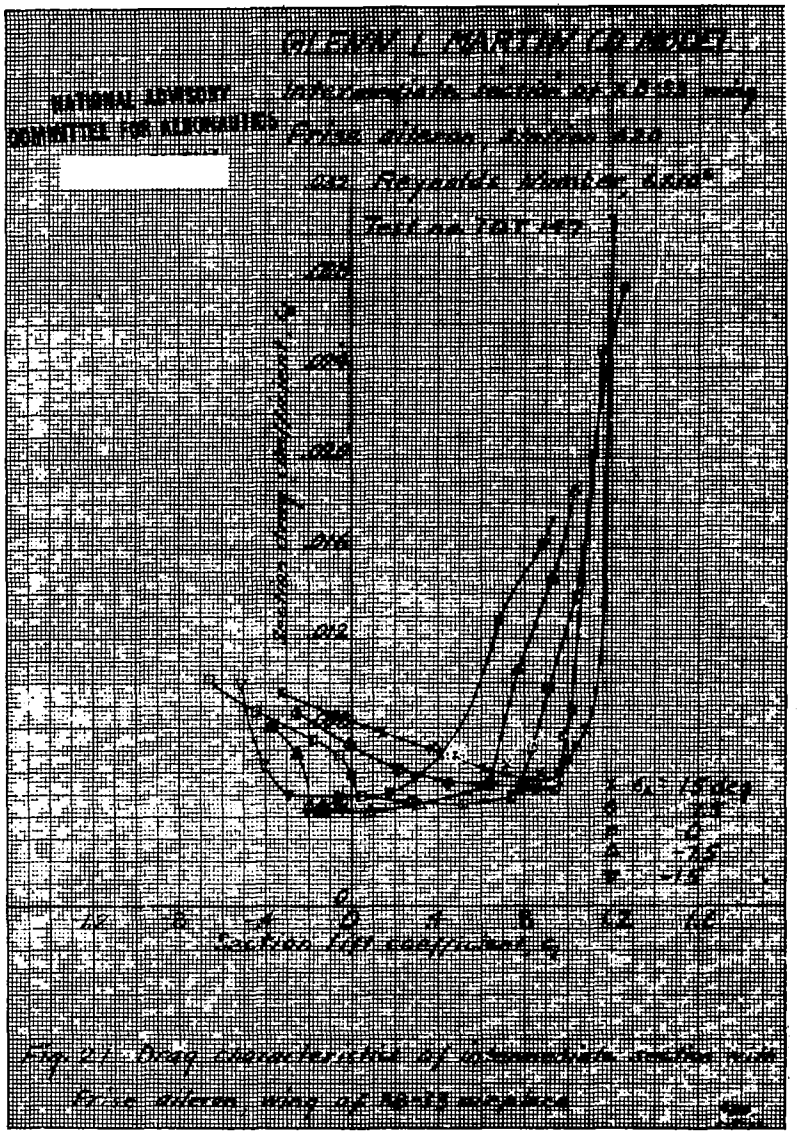

Fig. 21 Drag characteristics of intermediate section with frise aileron, wing of XB-33 airplane.

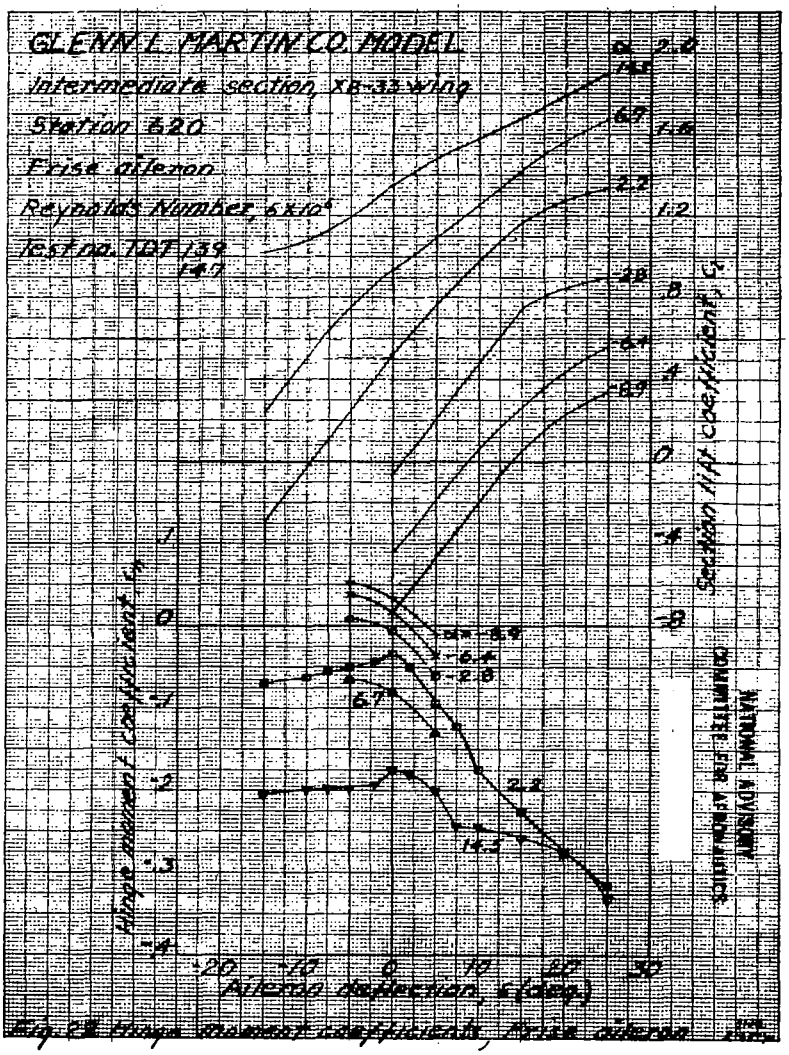

Fig. 28 Wing pitching moment coefficients, Frise aileron

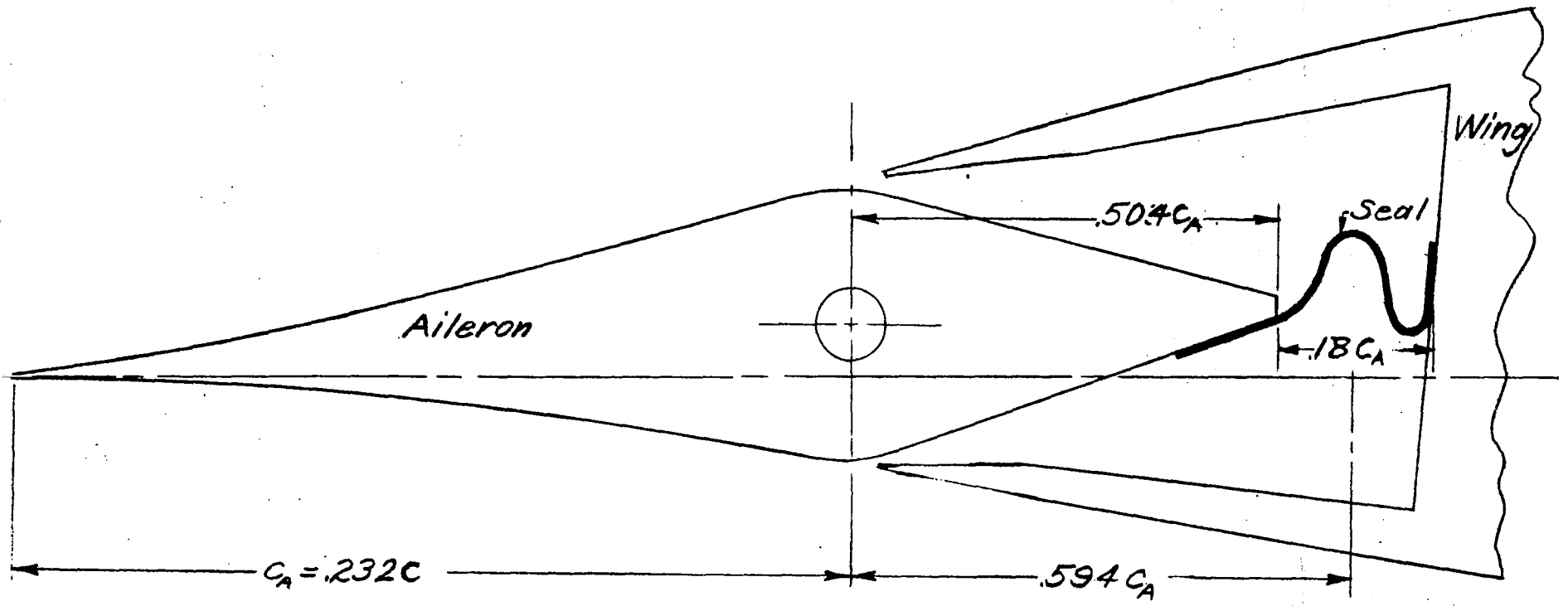

NATIONAL ADVISORY
COMMITTEE FOR AERONAUTICS

Fig. 23 Internal Balance Aileron

Glenn L. Martin Co. Model
Intermediate Section, XB-33 Wing

Station 620

Full Model Scale

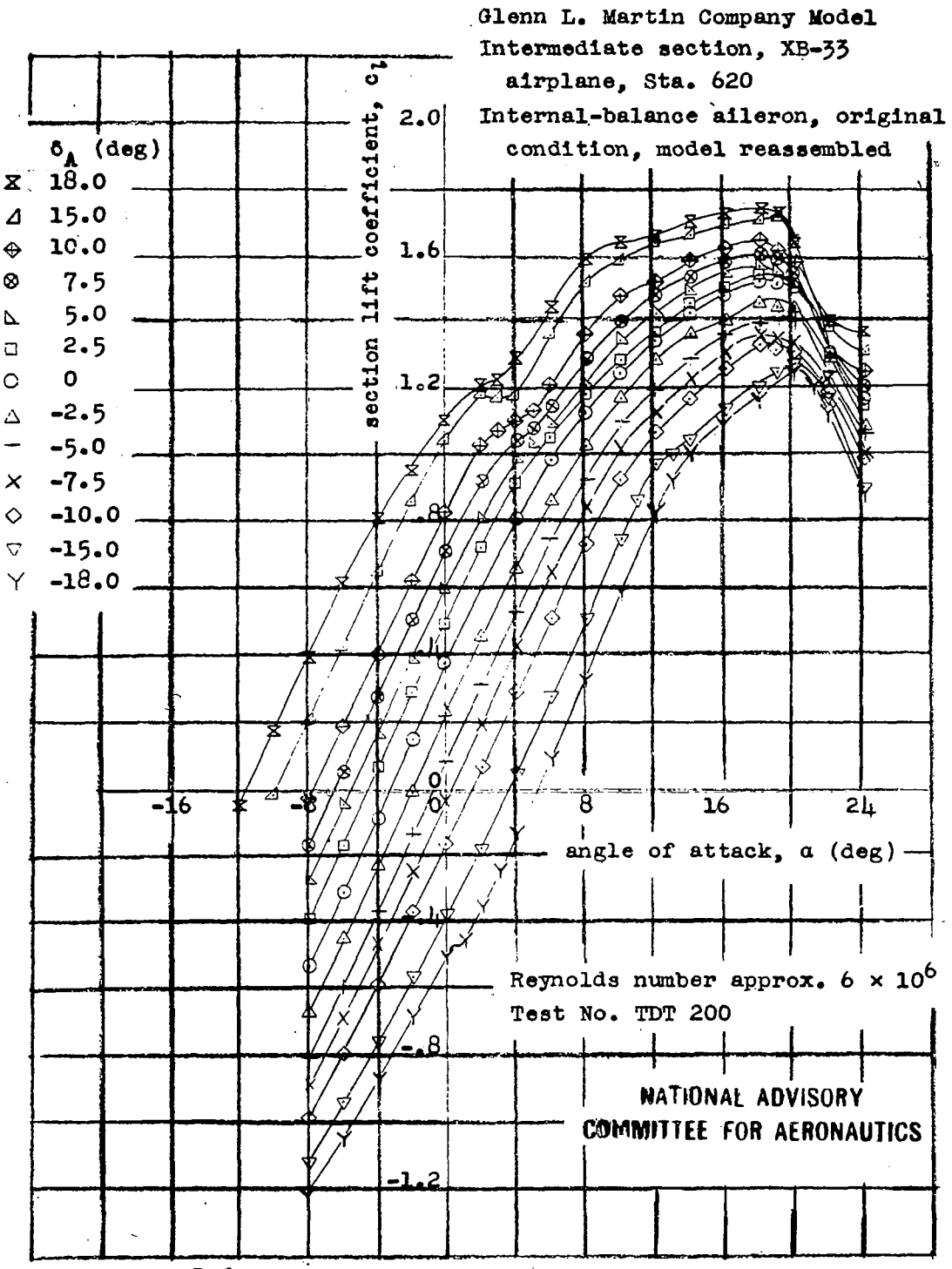

Figure 24 Lift characteristics of model with internal-balance aileron, original condition, model reassembled.

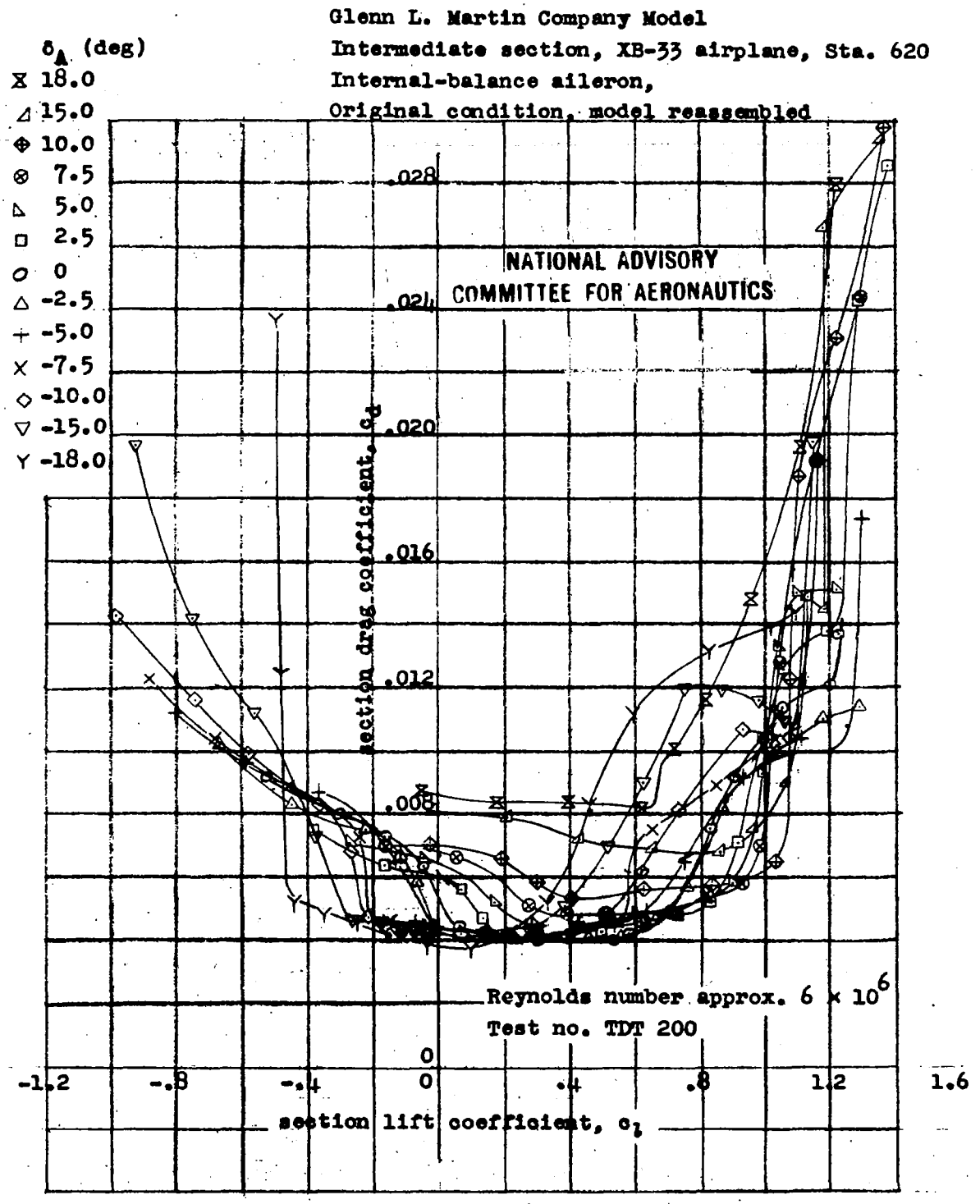

Figure 25 Drag characteristics of model with internal-balance aileron, original condition, model reassembled.

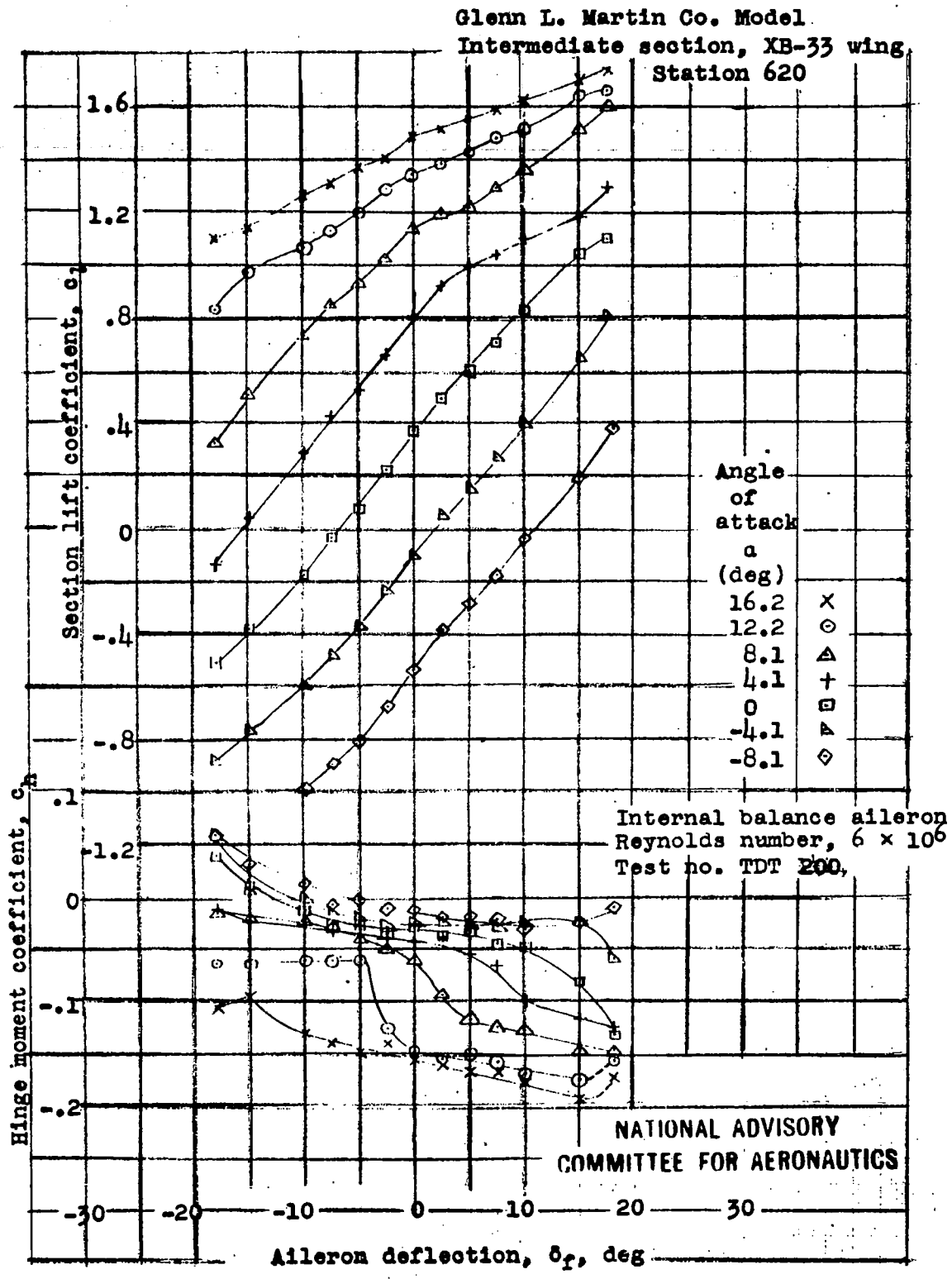

Figure 26.- Hinge moment coefficient, internal balance aileron.